


Heterogeneous Catalysis | Hot Paper |



Kasibhatta Josena Datta,^[a] Kasibhatta Kumara Ramanatha Datta,^[a] Manoj B. Gawande,^{*,[a]} Vaclav Ranc,^[a] Klára Čépe,^[a] Victor Malgras,^[b] Yusuke Yamauchi,^[b] Rajender S. Varma,^[c] and Radek Zboril^{*,[a]}

Abstract: A facile synthesis based on the addition of ascorbic acid to a mixture of Na₂PdCl₄, K₂PtCl₆, and Pluronic P123 results in highly branched core-shell nanoparticles (NPs) with a micro-mesoporous dandelion-like morphology comprising Pd core and Pt shell. The slow reduction kinetics associated with the use of ascorbic acid as a weak reductant and suitable Pd/Pt atomic ratio (1:1) play a principal role in the formation mechanism of such branched Pd@Pt core-shell NPs, which differs from the traditional seed-mediated growth. The catalyst efficiently achieves the reduction of a variety of olefins in good to excellent yields. Importantly, higher catalytic efficiency of dandelion-like Pd@Pt core-shell NPs was observed for the olefin reduction than commercially available Pt black, Pd NPs, and physically admixed Pt black and Pd NPs. This superior catalytic behavior is not only due to larger surface area and synergistic effects but also to the unique micro-mesoporous structure with significant contribution of mesopores with sizes of several tens of nanometers.

The synthesis of well-defined metal nanoparticles (NPs) with controlled morphology has been the prime focus of much research, owing to their interesting catalytic, electronic, photonic, and sensing properties.^[1] Various NPs with complex polyhedral morphologies featuring multiple compositions and high-index facets have been designed for both theoretical and experimental studies, revealing that the activity of NPs is de-

pendent on their size, shape, composition, and microstructure.^[2] Recently, numerous efforts have been made for the assembly of bimetallic NPs with a core-shell or an alloyed structure, given their remarkable catalytic properties that are often superior to those of their monometallic counterparts.^[3] Often, the addition of a second metallic component has a greater potential for enhancing the functionalities and performance of pure metal components due to significant synergistic effects.^[4]

Bimetallic core-shell NPs with well-defined shapes have been synthesized from noble metals such as Au, Pt, Pd, and Ag through heteroepitaxial growth of one metal on the surface of the other metal.^[5] For instance, a Pt monolayer supported on a Pd surface shows an improved activity for the oxygen reduction reaction (ORR) in comparison to the pure Pt surface.^[6] The interface between the Pd core and the Pt shell of Pd@Pt core-shell NPs provides a favorable environment for metal hydride formation, making this material useful for several applications. There are several strategies to prepare Pd@Pt core-shell NPs, including seed-mediated growth, co-reduction, and galvanic replacement.^[7]

Recently, particular attention has been focused on the fabrication of bimetallic core-shell NPs with highly branched/porous structures because of their promising catalytic and electronic properties. These assemblies exhibit high-index crystal facets on concave pore surfaces, defined as a set of Miller indices (*hkl*) with at least one integer higher than unity allowing easier access to active sites. More importantly, the porous framework allows the interaction or accessibility of reactants with more active surfaces due to the abundance of pores facilitating the overall kinetics of reaction.^[8] In continuation of ongoing research on core-shell NPs, especially as nanocatalysts, herein we describe a facile one-pot synthesis of porous and highly branched Pd@Pt core-shell NPs at room temperature without any organic solvents or addition of pre-synthesized seeds (Scheme 1).

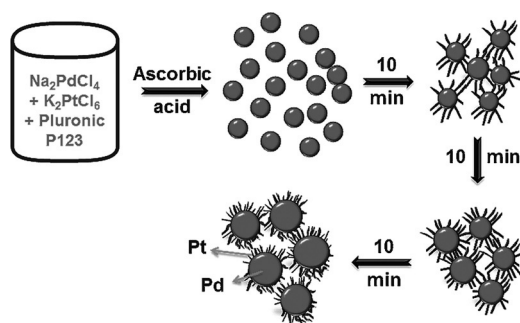
Interestingly, these nanoarchitectures displayed superior catalytic activity towards the reduction of olefins, an important reaction in organic chemistry, which is normally carried out by using hydrogen gas and heterogeneous transition metal catalysts.^[9] Complementary to catalytic hydrogenations with hydrogen gas, the use of cost-effective liquid hydrogen donors (transfer hydrogenation) allows the reduction process under ambient conditions without the use of high-pressure requirement. This is an alluring proposition in terms of safety issues as the requirement of flammable hydrogen gas (as for gas-

[a] K. J. Datta, Dr. K. K. R. Datta, Dr. M. B. Gawande, Dr. V. Ranc, Dr. K. Čépe, Prof. Dr. R. Zboril
Regional Centre of Advanced Technologies and Materials
Department of Physical Chemistry, Faculty of Science
Palacky University in Olomouc
Slechtitelu 27, Olomouc 78371 (Czech Republic)
E-mail: manoj.gawande@upol.cz
radek.zboril@upol.cz

[b] Dr. V. Malgras, Prof. Y. Yamauchi
World Premier International (WPI) Research Center for Materials
Nanoarchitectonics (MANA), National Institute for Materials Science (NIMS)
1-1 Namiki, Tsukuba, Ibaraki 305-0044 (Japan)

[c] Prof. R. S. Varma
Sustainable Technology Division, National Risk Management Research
Laboratory, US Environmental Protection Agency
26 West Martin Luther King Drive, MS 443, Cincinnati, Ohio, 45268 (USA)

Supporting information for this article is available on the WWW under <http://dx.doi.org/10.1002/chem.201503441>.



Scheme 1. Schematic illustration of the formation mechanism of Pd@Pt core-shell NPs.

phase hydrogenation reactions) can be avoided; liquid-phase hydrogen donors such as formic acid, ethanol, propanol, hydrazine hydrate, or ammonium formate can be deployed.^[10] An initial screening on the activity of Pd@Pt core-shell NPs for reduction of styrene revealed excellent catalytic activity in the presence of hydrazine hydrate as a reducing agent. Hydrazine hydrate is used in many organic syntheses with the only by-products being water and nitrogen gas.^[11]

The size and morphology of the as-prepared samples were characterized by transmission electron microscopy (TEM). The catalyst was composed of dandelion-like aggregates with highly porous structures and sizes ranging from 50–150 nm (Figure 1 a). Importantly, we did not observe any particles with

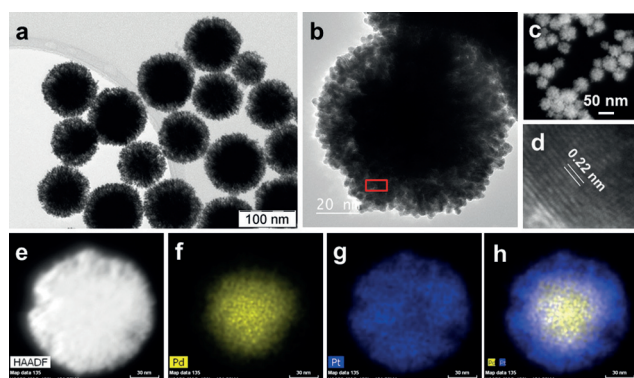


Figure 1. a) TEM and b) HRTEM images of the Pd@Pt NPs; c) HAADF-STEM image; d) HRTEM image of the highlighted region in (b); e) HAADF-STEM image of a single Pd@Pt nanoparticle; f–h) EDS elemental mapping showing the spatial distributions of Pd (f), Pt (g), and Pd–Pt (h).

out branched porous structures throughout the sample. A closer examination of the individual aggregate revealed the presence of well-defined branched shells (Figure 1 b). The high resolution (HR) TEM image clearly displayed that the NPs have a spherical core and uniformly branched shells, which was also observed by high-angle annular dark-field imaging scanning TEM (HAADF-STEM; Figure 1 c and e). The HRTEM of the particle in the surface shell shows the lattice spacing of 0.22 nm (Figure 1 d), which is commensurate with the (111) plane of the Pt fcc structure. Nanoscale elemental mapping on the individual aggregate distinctly revealed the uniform distribution of Pd

core and Pt shell, which further supports the formation of a highly organized porous core-shell Pd@Pt structure (Figure 1 e–f).

The wide-angle XRD pattern of Pd@Pt exhibits (111), (200), (220), (311), and (222) reflections that are consistent with the metallic face-centered-cubic (fcc) structure (see the Supporting Information, Figure S1 a). Most importantly the crystal structures (fcc) of Pd and Pt are similar with a very high lattice match (99.23%).^[12] The crystallite sizes calculated by Rietveld refinement are 12 and 3 nm for Pd and Pt NPs, respectively. Furthermore, selected-area electron diffraction (SAED) pattern (see the Supporting Information, Figure S1b) displayed rings assigned to fcc crystal structure, showing the polycrystalline nature of the Pd@Pt. The metallic nature and zero-valent state of both Pd and Pt NPs in the Pd@Pt composite were ascertained by X-ray photoelectron spectroscopy (XPS; see the Supporting Information, Figure S1c). The obtained binding energies at 71.42 and 74.75 eV correspond to $4f_{7/2}$ and $4f_{5/2}$ states of metallic Pt, whereas values at 335.73 and 340.99 eV correspond to $3d_{5/2}$ and $3d_{3/2}$ states of Pd.^[13] Finally, the cross-sectional compositional line profiles (see the Supporting Information, Figure S2) obtained through line scan confirm the dominant presence of Pd in the aggregate core, with Pt predominantly located in the surface shell of Pd@Pt nanoparticles. The atomic ratio of Pd to Pt estimated from atomic absorption spectroscopy (AAS) was found to be 1:1.

The mechanism of formation of the branched morphology of the Pd@Pt NPs was periodically investigated by time-sequential evolution experiments (Figure 2). Initially, NPs without

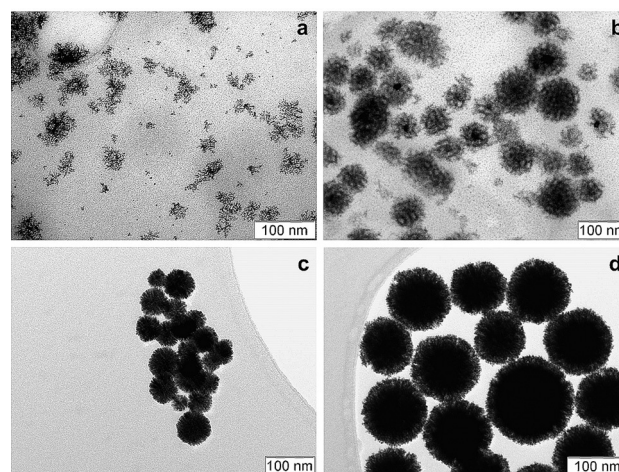
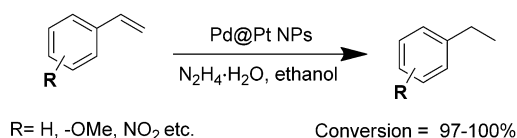


Figure 2. TEM images of Pd@Pt NPs collected during synthesis, after a) 1; b) 10; c) 20; d) 30 min.

branches were formed as soon as ascorbic acid was added to the metallic precursor in the presence of Pluronic P123 (a commercially available triblock copolymer; Figure 2 a). After 10 min, small NPs surrounding the dense core grew into branched nanostructures (Figure 2 b). Further progress in the reaction led to the formation of highly branched nanostructures, as evident from the samples collected after 20 and 30 min (Figure 2 c, d).

These observations revealed that the initially formed Pd NP seeds acted as nucleating centers for the formation of branch-like Pt nanostructures, reminiscent of structures previously reported by Zhou et al.^[14] We envisage that the swift separation of the Pd core and the Pt shell is due to the different reduction kinetics of their respective complexes formed with ascorbic acid. Due to the microscopic irregularities on the surface of the seeded NPs, the growth of the shell is anisotropic with the tips growing preferentially, culminating in the formation of branched nanoarchitectures. In the synthetic procedure, Pluronic P123 is crucial in generating the unique branched dandelion-like Pd@Pt NPs (see Experimental Section). Replacing P123 by cetyltrimethylammonium bromide (CTAB) produced large irregular aggregates composed of Pt and Pd NPs (see the Supporting Information, Figure S3 a). Similarly, replacement of ascorbic acid with the strong reducing agent sodium borohydride (NaBH₄) led to a poor geometrical assembly of Pd–Pt nanostructures, presumably due to the rapid reduction of metal species (see the Supporting Information, Figure S3 b), further elucidating the principal role of ascorbic acid in the formation of branched Pd@Pt NPs.

We next examined the catalytic efficacy of branched porous Pd@Pt NPs for the reduction of various olefins using hydrazine hydrate as a reducing agent at room temperature (Scheme 2).



Scheme 2. Olefin reduction catalyzed by Pd@Pt NPs.

The method has been found to have several advantages, such as low catalyst loading, shorter reaction times, and high product selectivity as compared to previously reported procedures.^[9a] In preliminary experiments, styrene was selected as a model substrate to optimize the reaction conditions. There was no appreciable reaction in the absence of catalyst (Table 1, entry 1). To compare the expected superior catalytic efficiency of the branched Pd@Pt NPs (Table 1, entry 2), commercially available Pt black and Pd NPs were employed for the reaction, using the same weight amount of NPs with hydrazine hydrate as hydrogen donor. It was noted that reaction remained incomplete, giving conversions of only 9% with Pd NPs and 4% with Pt black (Table 1, entries 3 and 4). Additionally, we investigated 2-propanol as a hydrogen donor. However, negligible conversion was obtained (Table 1, entry 5). Similarly, in the absence of hydrazine hydrate no conversion was registered (Table 1, entry 6). Thus, hydrazine hydrate was established as the best hydrogen source, when compared to 2-propanol in terms of conversion.

With optimized reaction conditions in hand, the substrate scope was examined. A variety of olefins bearing electron-withdrawing (4-fluoro, 3-nitro) or electron-donating (4-methoxy) substituents, were reduced to their corresponding products in

Table 1. Hydrogenation of styrene to ethylbenzene with hydrazine hydrate as a reducing agent promoted by various catalysts.^[a]

Entry	Catalyst	t [h]	Conversion [%] ^[b]
1	without catalyst	24	5
2	branched Pd@Pt (1:1)	0.5	100
3 ^[c]	Pd NPs	0.5	9
4 ^[c]	commercial Pt black	0.5	4
5 ^[d]	branched Pd@Pt (1:1)	2	6
6 ^[e]	branched Pd@Pt (1:1)	2	0

[a] Reaction conditions (unless otherwise stated): styrene (0.14 mmol), catalyst (2 mg), N₂H₄·H₂O (20 μL), aqueous NH₃ (10 μL, 28–30%), ethanol (1 mL), 60 °C; [b] conversion degree determined by gas chromatography; [c] catalyst (1 mg); [d] 2-propanol as hydrogen source; [e] without hydrazine hydrate.

Table 2. Reduction of various olefins catalyzed by Pd@Pt.^[a]

Entry	Substrate	Product	Conversion [%] ^[b]	Yield [%]
1			100	95
2			100	96
3			100	81
4			100 ^[c]	82
5			100	90
6			97 ^[d]	85

[a] Reaction conditions: Substrate (0.14 mmol), catalyst (2 mg), N₂H₄·H₂O (20 μL), aqueous NH₃ (10 μL, 28–30%), ethanol (1 mL), 60 °C for 30 min; [b] determined by gas chromatography; [c] at t = 60 min; [d] 94% ethylbenzene and 3% styrene after 60 min.

excellent conversions and yields (Table 2, entries 2–4), as was *trans*-stilbene (Table 2, entry 5). The reaction of phenylacetylene with hydrazine hydrate under the present experimental conditions afforded ethylbenzene as the major product alongside a very small amount of styrene (Table 2, entry 6).

Having already assessed the efficacy of Pd NPs and Pt black in the reduction of styrene as a model reaction (9% and 4% conversion, respectively; Table 1, entries 3 and 4), we also compared the catalytic activity of the developed branched core-shell Pd@Pt NPs with that of physically mixed Pd NPs and Pt black (Pd/Pt = 1:1) under the same reaction conditions (Figure 3). Whereas the individual metal components gave very poor conversions, we observed 20% conversion for the physically mixed Pd and Pt, in comparison to 100% conversion with

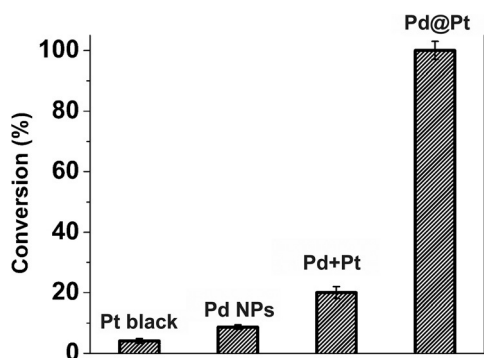


Figure 3. Comparison of the degree of conversion in the hydrogenation of styrene to ethylbenzene with Pt black, Pd NPs, a physical mixture of Pd and Pt NPs (1:1), and branched core-shell Pt@Pd NPs (1:1).

the Pd@Pt NPs. The Pd@Pt NPs' markedly higher catalytic activity than those of Pd NPs, Pt black and Pd+Pt NPs indicating the significant synergistic effects between the Pd core and Pt shell (Figure 3).

The improvement of the catalytic function of Pt catalysts by alloying with Pd is well known and has been reported in the literature^[4c,15] In the case of the core-shell (not alloyed) systems, the situation is quite different; core and shell elements play a critical role in determining the catalytic activity of the composite, as they can alter the binding energy of reaction intermediates on the NP surface.^[16] In addition, the effect of the surface area and the pore sizes of such hybrid systems needs to be stated, which might be among the major contributors in determining the catalytic activity because of the better transport of reactants/products. These parameters could be responsible for the extraordinary catalytic efficiency of the branched core-shell Pd@Pt NPs. Nitrogen adsorption-desorption isotherms and pore size distributions of the branched Pd@Pt NPs, Pd NPs, and commercial Pt black are given in the Supporting Information (Figure S4). The branched Pd@Pt NPs are shown to have a unique micro-mesoporous structure with a principal contribution of mesopores having sizes in tens of nanometers. Any mesoporous structure is considerably less developed or even absent for individual samples of Pd and Pt NPs. Thus, the considerably higher surface area and unique distribution of mesopores in the Pd@Pt catalyst, compared to Pd NPs and Pt black, offer better mass transport, which ultimately results in higher catalytic activity.

In summary, a facile one-pot aqueous synthetic method has been developed for the assembly of highly branched micro-mesoporous Pd@Pt core-shell NPs with unique dandelion-like morphology. This unique catalytic system could be achieved by the sequential formation of the Pd core followed by a Pt shell, owing to differences in their reduction kinetics associated with the use of ascorbic acid as a weak reducing agent. A wide range of functionalized olefins, such as 4-fluorostyrene and 4-methoxystyrene, were reduced in good to excellent yields by the branched Pd@Pt core-shell NPs with hydrazine hydrate as a hydrogen donor. The comparison of catalytic efficiency with individual metals (Pd NPs and commercial Pt black) and their physical mixture (Pd/Pt=1:1) for the reduction of styrene

showed that the developed branched core-shell Pd@Pt NPs stand out as the best candidate in terms of conversion, owing to synergistic effects of the combination of Pd and Pt. We believe that unique micro-mesoporous structure, with a high contribution from mesopores, is one of the key parameters responsible for the superior catalytic activity. Indeed, we envisage the applicability of Pd@Pt nanoarchitectures as a promising material for various catalytic organic transformations, energy storage and fuel-cell technologies.

Experimental Section

Typical synthesis of Pd@Pt core-shell NPs

To a stirred solution of K_2PtCl_6 (17.5 mM), Na_2PdCl_4 (2.5 mM), and Pluronic P123 (1.74 mM) in water (5 mL) was quickly added 0.1 M ascorbic acid (AA, 5 mL) and the resultant mixture was stirred for 30 min at room temperature. The color of the solution immediately changed from transparent brownish to dark brownish-red and finally to opaque black. After 30 min of reaction, the product was isolated and residual Pluronic P123 was removed by centrifugation at 8000 rpm for 20 min, followed by three consecutive washing/centrifugation cycles with water (120 mL). The collected product was dried at 50 °C and/or redispersed in water by sonication to produce a colloidal suspension for further characterization.

Acknowledgements

The authors thank Ms. J. Straska for TEM, Mr. M. Petr for XPS, Dr. C. Aparicio for XRD, Mr. M. Krizek for porosity and adsorption-desorption measurements, and Dr. J. Tucek for technical assistance. The authors acknowledge support from the Ministry of Education, Youth and Sports of the Czech Republic (LO1305) and the Operational Program Education for Competitiveness: European Social Fund (projects CZ.1.07/2.3.00/30.0041 and CZ.1.07/2.3.00/30.0004).

Keywords: core-shell nanoparticles · heterogeneous catalysis · olefins · palladium · platinum reduction

- [1] a) A. C. Chen, P. Holt-Hindle, *Chem. Rev.* **2010**, *110*, 3767–3804; b) X. Q. Huang, Y. J. Li, Y. Chen, E. B. Zhou, Y. X. Xu, H. L. Zhou, X. F. Duan, Y. Huang, *Angew. Chem. Int. Ed.* **2013**, *52*, 2520–2524; *Angew. Chem.* **2013**, *125*, 2580–2584.
- [2] a) S. E. Habas, H. Lee, V. Radmilovic, G. A. Somorjai, P. Yang, *Nat. Mater.* **2007**, *6*, 692–697; b) L. Wang, Y. Yamauchi, *J. Am. Chem. Soc.* **2009**, *131*, 9152–9153; c) B. Lim, Y. N. Xia, *Angew. Chem. Int. Ed.* **2011**, *50*, 76–85; *Angew. Chem.* **2011**, *123*, 78–87.
- [3] a) M. B. Gawande, A. Goswami, T. Asefa, H. Guo, D.-L. Peng, A. Biradar, R. Zboril, R. S. Varma, *Chem. Soc. Rev.* **2015**, *44*, 7540–7590; b) R. Ghosh Chaudhuri, S. Paria, *Chem. Rev.* **2012**, *112*, 2373–2433; c) C. Burda, X. B. Chen, R. Narayanan, M. A. El-Sayed, *Chem. Rev.* **2005**, *105*, 1025–1102; d) X. W. Liu, X. G. Liu, *Angew. Chem. Int. Ed.* **2012**, *51*, 3311–3313; *Angew. Chem.* **2012**, *124*, 3367–3369; e) Y. Ding, F. R. Fan, Z. Q. Tian, Z. L. Wang, *J. Am. Chem. Soc.* **2010**, *132*, 12480–12486.
- [4] a) D. S. Wang, Y. D. Li, *Adv. Mater.* **2011**, *23*, 1044–1060; b) H. Yang, *Angew. Chem. Int. Ed.* **2011**, *50*, 2674–2676; *Angew. Chem.* **2011**, *123*, 2726–2728; c) H. Zhang, M. S. Jin, Y. N. Xia, *Chem. Soc. Rev.* **2012**, *41*, 8035–8049; d) F. Zaera, *Chem. Soc. Rev.* **2013**, *42*, 2746–2762; e) Q. Zhang, I. Lee, J. B. Joo, F. Zaera, Y. D. Yin, *Acc. Chem. Res.* **2013**, *46*, 1816–1824; f) H. Wang, L. Y. Chen, Y. H. Feng, H. Y. Chen, *Acc. Chem.*

- Res. **2013**, *46*, 1636–1646; g) S. G. Zhou, K. McIlwrath, G. Jackson, B. Eichhorn, *J. Am. Chem. Soc.* **2006**, *128*, 1780–1781.
- [5] a) Y. J. Li, Z. W. Wang, C. Y. Chiu, L. Y. Ruan, W. B. Yang, Y. Yang, R. E. Palmer, Y. Huang, *Nanoscale* **2012**, *4*, 845–851; b) B. Lim, J. G. Wang, P. H. C. Camargo, M. J. Jiang, M. J. Kim, Y. N. Xia, *Nano Lett.* **2008**, *8*, 2535–2540.
- [6] a) J. W. Hong, S. W. Kang, B. S. Choi, D. Kim, S. B. Lee, S. W. Han, *ACS Nano* **2012**, *6*, 2410–2419; b) H. Zhang, Y. J. Yin, Y. J. Hu, C. Y. Li, P. Wu, S. H. Wei, C. X. Cai, *J. Phys. Chem. A J. Phys. Chem. B J. Phys. Chem. C* **2010**, *114*, 11861–11867.
- [7] a) P. P. Zhang, Y. B. Hu, B. H. Li, Q. J. Zhang, C. Zhou, H. B. Yu, X. J. Zhang, L. Chen, B. Eichhorn, S. H. Zhou, *ACS Catal.* **2015**, *5*, 1335–1343; b) B. Lim, M. J. Jiang, P. H. C. Camargo, E. C. Cho, J. Tao, X. M. Lu, Y. M. Zhu, Y. N. Xia, *Science* **2009**, *324*, 1302–1305; c) M. J. Jiang, B. Lim, J. Tao, P. H. C. Camargo, C. Ma, Y. M. Zhu, Y. N. Xia, *Nanoscale* **2010**, *2*, 2406–2411; d) H. Zhang, M. S. Jin, J. G. Wang, M. J. Kim, D. R. Yang, Y. N. Xia, *J. Am. Chem. Soc.* **2011**, *133*, 10422–10425; e) B. Lim, J. G. Wang, P. H. C. Camargo, C. M. Copley, M. J. Kim, Y. N. Xia, *Angew. Chem. Int. Ed.* **2009**, *48*, 6304–6308; *Angew. Chem.* **2009**, *121*, 6422–6426; f) Y. Liu, M. F. Chi, V. Mazumder, K. L. More, S. Soled, J. D. Henao, S. H. Sun, *Chem. Mater.* **2011**, *23*, 4199–4203; g) H. Kobayashi, M. Yamauchi, H. Kitagawa, Y. Kubota, K. Kato, M. Takata, *J. Am. Chem. Soc.* **2008**, *130*, 1818–1819; h) S. F. Xie, S. I. Choi, N. Lu, L. T. Roling, J. A. Herron, L. Zhang, J. Park, J. G. Wang, M. J. Kim, Z. X. Xie, M. Mavrikakis, Y. N. Xia, *Nano Lett.* **2014**, *14*, 3570–3576; i) Y. Wang, N. Tushima, *J. Phys. Chem. B* **1997**, *101*, 5301–5306.
- [8] a) L. Wang, Y. Nemoto, Y. Yamauchi, *J. Am. Chem. Soc.* **2011**, *133*, 9674–9677; b) L. Wang, Y. Yamauchi, *J. Am. Chem. Soc.* **2010**, *132*, 13636–13638; c) L. Wang, Y. Yamauchi, *Chem. Mater.* **2011**, *23*, 2457–2465.
- [9] a) A. Dhakshinamoorthy, S. Navalon, D. Sempere, M. Alvaro, H. Garcia, *Chem. Commun.* **2013**, *49*, 2359–2361; b) C. Smit, M. W. Fraaije, A. J. Minnaard, *J. Org. Chem.* **2008**, *73*, 9482–9485.
- [10] a) R. V. Jagadeesh, G. Wienhofer, F. A. Westerhaus, A. E. Surkus, H. Junge, K. Junge, M. Beller, *Chem. Eur. J.* **2011**, *17*, 14375–14379; b) S. Horn, C. Gandolfi, M. Albrecht, *Eur. J. Inorg. Chem.* **2011**, 2863–2868; c) S. Gladioli, E. Alberico, *Chem. Soc. Rev.* **2006**, *35*, 226–236; d) P. S. Kumbhar, J. Sanchez-Valente, J. M. M. Millet, F. Figueras, *J. Catal.* **2000**, *191*, 467–473; e) S. M. Auer, J. D. Grunwaldt, R. A. Koppel, A. Baiker, *J. Mol. Catal. A* **1999**, *139*, 305–313; f) R. Kadyrov, T. H. Riermeier, *Angew. Chem. Int. Ed.* **2003**, *42*, 5472–5474; *Angew. Chem.* **2003**, *115*, 5630–5632.
- [11] a) M. Benz, R. Prins, *Appl. Catal. A* **1999**, *183*, 325–333; b) Y. J. Gao, D. Ma, C. L. Wang, J. Guan, X. H. Bao, *Chem. Br. Chem. Commun.* **2011**, 47, 2432–2434; c) A. K. Jain, *Synlett* **2004**, 2445–2446; d) M. Lauwiner, P. Rys, J. Wissmann, *Appl. Catal. A* **1998**, *172*, 141–148; e) P. G. Ren, D. X. Yan, X. Ji, T. Chen, Z. M. Li, *Nanotechnology* **2011**, *22*, 055705; f) U. Sharma, P. Kumar, N. Kumar, V. Kumar, B. Singh, *Adv. Synth. Catal.* **2010**, *352*, 1834–1840.
- [12] a) L. Wang, Y. Yamauchi, *J. Am. Chem. Soc.* **2013**, *135*, 16762–16765; b) H. Atae-Esfahani, M. Imura, Y. Yamauchi, *Angew. Chem. Int. Ed.* **2013**, *52*, 13611–13615; *Angew. Chem.* **2013**, *125*, 13856–13860.
- [13] Y. Z. Lu, Y. Y. Jiang, W. Chen, *Nano Energy* **2013**, *2*, 836–844.
- [14] Y. X. Zhou, D. S. Wang, Y. D. Li, *Chem. Commun.* **2014**, *50*, 6141–6144.
- [15] H. J. Lee, S. E. Habas, G. A. Somorjai, P. D. Yang, *J. Am. Chem. Soc.* **2008**, *130*, 5406–5407.
- [16] a) R. Choi, S. I. Choi, C. H. Choi, K. M. Nam, S. I. Woo, J. T. Park, S. W. Han, *Chem. Eur. J.* **2013**, *19*, 8190–8198; b) P. Strasser, S. Koh, T. Anniyev, J. Greeley, K. More, C. F. Yu, Z. C. Liu, S. Kaya, D. Nordlund, H. Ogasawara, M. F. Toney, A. Nilsson, *Nat. Chem.* **2010**, *2*, 454–460; c) W. J. Tang, G. Henkelman, *J. Chem. Phys.* **2009**, *130*, 194504.

Received: August 29, 2015

Published online on November 13, 2015